Supplementary materials for:

Representative estimates of covid-19 infection fatality rates from four locations in India: cross-sectional study

Rebecca Cai, Paul Novosad, Vaidehi Tandel, Sam Asher, Anup Malani*

* Correspondence to: amalani@uchicago.edu

This PDF file includes:

Detailed Materials and Methods
eFigures 1 to 9
eTables 1 to 6

Materials and Methods

Bihar

Data

We made use of data on all positive cases in the state of Bihar found during random testing of incoming migrants during an early phase of the pandemic. The data was provided by the Health Department of the Government of Bihar. The data contained a sample of 4,954 active infections and their outcomes, reported between March 22 (the date on which the first positive case in Bihar was detected) and July 21, 2020. The vast majority of the sample (over 99%) consisted of migrants travelling from within India into Bihar, most on designated trains. Migrants were more likely to be sampled if they presented symptoms between March 22 and May 3. State policy beginning May 4 during the sample collection period mandated that travellers from within or outside India (mainly migrant workers returning home due to travel restrictions) be randomly sampled and tested for COVID-19 infection from March 20 to May 22, and after May 31. Between May 22–31, only migrants from seven high-infection cities (National Capital Region, Mumbai, Ahmedabad, Pune, Surat, Kolkata, and Bangalore) in India were randomly sampled. We isolated the subsample of migrants who were randomly selected for testing, yielding 4,362 cases.

During the sample period, migrants were tested with TrueNat machines manufactured by MolBio Diagnostics in Goa (India), and positive tests were confirmed with real-time reverse polymerase chain reaction (RT-PCR) kits (CMO-PRC, 2020). Importantly, all infected migrants were tracked by the monitoring team, to determine whether they eventually recovered or died. Among randomly sampled male migrants, 1,385 infected individuals (35%), whom we call "lost", could not be tracked and thus their final outcome is uncertain. The high level of attrition is common in studies of migrant workers, whose frequent movement complicates administrative registration and tracking, particularly during a crisis (Deshingkar et al., 2008). We considered several approaches to adjusting for attrition, described below. The migrant sample, reflecting typical labor migration patterns in India, was overwhelmingly male (90%). Thus we limited our final analytical sample to 3,921 randomly sampled male migrants, for 2,536 of whom outcomes (recovery or death) are known.

Estimating infection fatality rate

Because everyone in the sample had tested positive for SARS-CoV-2, IFRs were estimated as the share of deaths among non-lost individuals in each age group. To account for potential biases due to attrition and delays between infection and recovery/death/reporting, we estimated IFRs using three separate methods, and report estimates from all three.

In age group a, denote the number of lost cases as $n_{a,lost}$, the number of recovered cases as $n_{a,recovered}$, and the number of cases ending in death as $n_{a,died}$.

Method 1 (main estimation): In our main estimation, we assumed that lost cases had the same IFR as successfully tracked cases, within each age group. This assumption was implemented by excluding lost individuals from the IFR calculation. Method 1 provided a midline IFR estimate:

$$IFR1_a = \frac{n_{a,died}}{n_{a,died} + n_{a,recovered}}$$

Method 2: In this estimation, we assumed that all lost cases eventually recovered. Thus Method 2 provided a lower bound IFR estimate:

$$IFR2_a = \frac{n_{a,died}}{n_{a,died} + n_{a,recovered} + n_{a,lost}}$$

Method 3: The share of cases with successful followup declined in late July as the volume of migrants increased. In the third method, to account for potential right-censoring of reported outcome rate due to delays between report of initial infection and report of recovery/death, we dropped all cases reported within two weeks of the last report date (July 21st):

$$IFR3_a = \left(\frac{(n_{a,died})}{n_{a,died} + n_{a,recovered} + n_{a,lost}} \middle| \text{ infection reported on or before July 7}\right)$$

Standard errors were estimated with the normal approximation for a proportion from multiple draws from a binomial distribution.

Mumbai

Data

Data on seroprevalence were obtained from a representative, stratified, random sample of slum and non-slum populations in three of twenty-four wards of Mumbai (see Malani et al. (2020) for full survey design). Sample collection lasted two weeks and ended on July 14th in slums and July 19th in non-slums. The three wards were selected to represent the city's three broad zones (city, eastern suburbs, western suburbs); choice of sampled ward within each zone was by convenience. The sample consists of 6,904 participants (4,202 from slums and 2,702 from non-slums), who were tested for IgG antibodies to the SARS-CoV-2 N-protein using the Abbott Diagnostics Architect^{TM} N-protein based test. The samples were stratified by four age groups, sex, ward, and slum/non-slum residence.

Data on reported infections and deaths by ward and age distribution of deaths were provided in reports released by the municipal governing body (Brihanmumbai Municipal Corporation, hereafter BMC). Data on ward population in slums and non-slums came from the 2011 Population Census. Data on shares of population by age and sex in each ward-slum came from the 2012 Socio-Economic and Caste Census.

Estimating IFR

Estimating number of infections. The seroprevalence survey reported seropositivity in four age groups (12–24, 25–39, 40–60, 61+), called "coarse bins". To generate infection counts that could be compared with city death statistics (which are reported in 10-year age bins), seropositivity by 10-year age bin was interpolated by fitting a non-linear function over seropositivity in the coarse bins. For the main estimation, we interpolated seropositivity in 10-year bins, using the inverse distance-weighted mean of non-missing values (using the Stata package mipolate), weighting with the squared inverse of distance. In each coarse bin, the median age of residents in Mumbai City was used as the non-missing value for age. As a sensitivity analysis, we report IFR estimates using a piecewise cubic Hermite ("pchip") interpolation for seropositivity. Interpolation predicted seroprevalence for the midpoint of each 10-year age bin, separately by sex, ward, and slum status.

The estimated sensitivity of the chemiluminiscence immunoassay ranges from 90% (95% CI: 74 to 96) (USFDA, 2020) to 96% (89 to 99) (Bryan et al., 2020) while specificity in those studies was 100% (95% CI: 95 to 100) and 99.0%, respectively. We estimated seroprevalence from seropositivity using the Rogan-Gladen correction (Rogan and Gladen, 1978) to account for imperfect accuracy of tests. In the main results, we used the midpoint of mean sensitivity estimates (93.5%) and the midpoint of corresponding specificities (99%). As a sensitivity analysis, we replicated results with an upper bound for seroprevalence based on the Abbott test's lower bound of sensitivity (90%) and upper bound of specificity (100%) (Bryan et al., 2020) (Figure 4).

Denote the estimated number of infections in age bin a, sex g in sampled ward s as:

$$\widehat{inf}_{ags} = SP_{ags} \times pop_{ags}$$

where $SP_{ag,s}$ is the estimated seroprevalence rate, and $pop_{ag,s}$ is population.

Estimating the number of infections in non-sampled wards. BMC death data reported the ward of death, but not the ward of residence. Discussion with government officials and review of the data indicated that the ward of death was not a reliable indicator of ward of residence. This implied that calculating IFR by dividing the number of ward-level deaths by the number of ward-level infections would overestimate deaths in wards with large hospitals and underestimate them elsewhere. Instead, we used the seroprevalence surveys to generate estimates of city-wide infection counts.

To estimate true number of infections in non-sampled wards, we drew on administrative ward-level infection counts (which were universally available from city reports), and assumed that the BMC underestimated the true population infection count at the same rate in sampled and non-sampled wards within the same zone. This assumption is supported by Table 1, which shows that in the three wards where we obtained seroprevalence data, case multipliers were very similar.

Thus, in each zone z, we calculated a case multiplier based on sampled ward s:

$$\gamma_z = \frac{\sum_a \sum_g \widehat{inf}_{ag,s}}{\text{BMC-reported cases}_s}$$

The multiplier indicates the under-reporting rate in each zone z. The numerator of the expression is calculated from the seroprevalence surveys as above, and the denominator is taken from the BMC reports. BMC-reported cases were measured as of July 19, the last day of seroprevalence sample collection. We then multiplied the BMC's reported number of positive cases in non-sampled ward n in zone z by γ_z. That is,

$$\widehat{inf}_{n,z} = \gamma_z \times \text{BMC-reported cases}_n$$

The benefit of this approach is that it allows pandemic intensity to vary across wards, a realistic assumption given significant ward-level variation in reported cases per capita and number of containment zones.

This approach also implicitly assumes that the BMC under-reports cases in slums and non-slums at the same rate, *i.e.* a ward's case multiplier does not depend on share of population living in slums. This assumption is also supported by the consistent multipliers reported in Supplement Table 1, across three wards with different slum shares.

Estimating the number of infections in each age-sex group in non-sampled wards. We did not observe the age and sex distribution of infections outside of the sampled wards, so it was necessary to assume that non-sampled wards had the same age and sex distribution of infections of sample wards. This was supported by similar age and sex distributions of infections in the three wards with seroprevalence surveys. Figure 9 shows the calculated age and sex distribution of infections; note that the distribution of infections measured with seroprevalence skews younger than the number of reported positive cases, which we presume omits many infected but asymptomatic young people. This approach would cause error if the age distribution varied substantially across wards, but it is overall quite similar; even the median age gap between slums and non-slums was less than one year.

The number of infections in non-sampled ward s for sex g in age a was thus calculated as:

$$\widehat{inf}_{ag,n} = \frac{\sum_s \alpha_{ag,s}}{\sum_s \sum_a \sum_g \alpha_{ag,s}} \times \widehat{inf}_n,$$

where $\alpha_{ag,s}$ is the age-sex group's share of total cases in sampled ward s.

Estimating the number of deaths. To map infection counts to death counts, we must make assumptions about the delays between infection and death and between infection and seroprevalence. The literature suggests the distribution of delay between symptom onset and death (Linton et al., 2020) that is wider than that between onset and seroconversion (Stringhini et al., 2020). Linton et al. estimated a median time delay of 13 days (17 days with right truncation) between illness onset to death. Stringhini et al. estimated a mean delay of 11. days between symptom onset and seroconversion. Based on these estimates, we assumed that the delay between infection and death is on average two days longer than the delay between infection and seroconversion. In the main results, the number of deaths was therefore measured as the cumulative deaths reported in each Mumbai ward as of July 21. This is likely to slightly overstate the IFR, since some deaths may have been associated with individuals who contracted the virus after testing negative in the seroprevalence surveys. However, this upward bias is partially balanced out by the fact that the time between seroconversion and death is not uniform and is likely to be longer than 2 days for a non-trivial share of cases.

Rather than model non-uniform delays between infection and death, we bounded our IFR estimates from above by choosing more conservative death dates. In sensitivity analyses reported below (Figure 1), we replicated IFR estimates using deaths from one week (July 28) and two weeks (August 4) after the end of seroprevalence surveying, both of which plausibly overestimated the number of deaths related to the seroprevalence surveys, given the context of steadily increasing case counts in Mumbai from June to August.

The assumption that deaths measured 1 and 2 weeks later will lead to upward biased IFRs is further strengthened by recent evidence from roughly 125,000 cases in two other Indian states (Laxminarayan et al., 2020), which found that delays between case report and death were significantly shorter than delays found in China and the United States (Lewnard et al., 2020).

We used the age distribution of deaths as reported by the BMC up to the date used for measuring deaths, and the sex distribution (65% male, 35% female) up to August 3 (Debroy, 2020) (the sex distribution of deaths was not included in earlier reports). This yields the estimated number of city-wide deaths by age-sex group, d_{ag}.

Estimating city-wide IFR by age in Mumbai. Denote the final city-wide IFR in Mumbai, in age bin a for sex g, as IFR_{ag}:

$$IFR_{ag} = \frac{d_{ag}}{\sum_{ns} \widehat{inf}_{ag,ns} + \sum_s \widehat{inf}_{ag,s}}$$

Standard errors of IFRs were calculated reflecting propagation of the design-based standard errors of the age- and sex-specific seroprevalence estimates with a normal approximation.

Karnataka

Data

Data on seroprevalence were obtained from the Karnataka Seroprevalence Survey (hereafter KSS) a state-wide representative sample of urban and rural areas in 20 out of 30 districts in Karnataka, representing 5 broader regions (see Mohanan et al. (2021) for a detailed survey description). The sample was collected from June 15 to August 29, 2020. Collection times within individual regions were significantly shorter. The study sample was drawn from an existing representative sample of a panel survey—the Consumer Pyramids Household Survey (CPHS)—collected by the Center for Monitoring Indian Economy (CMIE). Our analytical subsample consists of 1,196 tests for IgG antibodies to the receptor binding domain (RBD) of the SARS-CoV-2 virus using an ELISA test developed by Translational Health Science and Technology Institute, India. The sample was not stratified by age and sex, an issue addressed below.

Data on confirmed COVID-19 deaths by district were drawn from Government of Karnataka Department of Health and Family Welfare bulletins, which are released several times per week. Data on the age distribution of total COVID-19 deaths were given by public reports from the state COVID-19 task force. Data on the sex distribution of deaths by age group were obtained from an individual-level dataset of confirmed COVID-19 deaths which was updated through July. The case-level death data were parsed from covid19india.org. Age- and sex-disaggregated population for districts and regions was drawn from the 2012 Socio-Economic and Caste Census (SECC).

Estimating IFR

Estimating the number of infections. The KSS dataset was designed to be representative of 5 broader regions in Karnataka. We therefore can take the ELISA positive test rate as an unbiased measure of the region-level positivity rate. We pooled the data across regions to obtain a statewide test positivity rate in each age and sex group, weighting by region population in each age-sex group.

We then corrected for the sensitivity (84%) and specificity (100%) of the ELISA imunoassay (Chaudhuri et al., 2020), using the Rogan-Gladen correction (Rogan and Gladen, 1978). This yielded the estimated seroprevalence by age-sex group SP_{ag}, which is multiplied by population pop_{ag} in each age-sex bin to generate an estimated number of infections $\widehat{inf}_{ag}$, as was done in Mumbai.

Estimating the number of deaths. The seroprevalence samples were collected at different times in different regions, with the survey period spanning roughly two months (Table 2). To estimate an IFR, we need to match the timing of deaths to the timing of seroprevalence surveying in each region.

Choice of dates for measuring deaths. As in Mumbai, we worked from an assumption that the average time difference between seroconversion and death was two days, while testing sensitivity to alternate assumptions (Figure 2). We therefore matched the estimated number of infections calculated in each region to the number of deaths recorded in administrative data two days after the last date of seroprevalence surveying. As in Mumbai, if the two-day delay between seroconversion and death was uniform, this approach would overestimate the IFR, because it counts the deaths of some people who may have been infected *after* recording negative seroprevalence tests.

In all regions except Bangalore, seroprevalence surveying was conducted over a three week period or less, making it straightforward to match test data to death data. In Bangalore, surveying was begun in mid-June but was interrupted by a lockdown. Survey teams returned to finish sampling in the last week of August. Matching Bangalore deaths to the last date of seroprevalence surveying is therefore likely to overestimate the IFR, because a number of those deaths may have been associated with individuals contracting SARS-CoV-2 after testing negative. It was not possible to disaggregate the early and late surveys because death reporting was at the district level, and the early and late survey groups were not representative in and of themselves. To adjust for increased uncertainty regarding the number of infections in Bangalore, we therefore report a sensitivity analysis for all of Karnataka excluding Bangalore (Figure 5).

On some days, official deaths were not reported; in those cases, we used deaths from the following day.[1]

Estimating the number of deaths in each demographic group: The Karnataka state government released total death counts on a daily basis, but only intermittently published the age distribution of state-wide deaths. To attribute daily deaths to age and sex groups, we used the age distribution of deaths from the nearest available date. The longest period between the date used for deaths and the date used for age-shares was 13 days.

Government reports provided age shares of deaths in 10-year bins in the form (e.g.) 51-60, while the seroprevalence surveys provided age bins in the form (e.g.) 50-59. To harmonize the age groups, we use the medians of the provided bins (e.g. median of 51-60 is 55.) to interpolate death data to match the age bins in the seroprevalence data, using an inverse distance weighted average method via the mipolate Stata package. Because the target age bins were very close to the available age bins, the risk of error here is small. As a sensitivity test, we replicated IFRs using piecewise cubic Hermite interpolation. For more details, see the discussion on interpolation in Mumbai.

[1] In Belgaum, the target date was July 27th; we used July 28. In the sensitivity test, the target date was August 10; we used August 11.

In the absence of death data disaggregated by age and sex on most dates, we assumed that, within age group, the sex distribution of deaths was uniform across regions and equal to the state-wide sex distribution of deaths reported between April and July. This assumption is supported by the finding that IFRs among males were approximately double those among females, consistent with reports from other countries.

Standard errors of IFRs reflect propagation of design-based standard errors of the age- and sex-specific seroprevalence estimates with a normal approximation.

Tamil Nadu

Data

Data on seroprevalence in Tamil Nadu comes from a state-conducted population-level seroprevalence survey of 26,640 adults aged 18 and older, covering the 37 districts of the state. The sample was collected between October 19 and November 30, 2020. Collection times within districts were often significantly shorter. The sampling frame divided Tamil Nadu's 37 administrative districts (as of February 2020) into health unit districts (HUDs), then formed and randomly sampled urban and rural clusters. Within clusters, enumerators started at a randomly selected GPS starting point, sampling one person from households adjacent to the starting point (using the Kish method) to provide a biosample, until 30 persons were sampled per cluster. Serum was analyzed for IgG antibodies to the SARS-CoV-2 spike protein using either the iFlash-SARS-CoV-2 IgG (Shenzhen YHLO Biotech; sensitivity of 95% and specificity of 95% per manufacturer (Shenzhen YHLO Biotech No. Ltd., 2020)) or the Vitros anti-SARS-CoV-2 IgG CLIA kit (Ortho- Clinical Diagnostics; sensitivity of 90% and specificity of 100% per manufacturer). For uniformity, in each district, one type of kit was used; in one district (Chennai) both kits were used. Our analytical subsample consists of 26,107 CLIA antibody tests that could be conclusively determined as positive or negative.

Case-level data on state-wide COVID-19 deaths was collected from daily government reports released on https://stopcorona.tn.gov.in/daily-bulletin/. The data cover all recorded deaths, beginning on March 25 and updated until December 24, 2020. The data was collected and shared by the faculty and staff of the Urban Expansion Observatory at Pillai College, New Panvel, Maharashtra. The dataset contains 12,019 observations, each with information about age, sex, dates of reported positive test and death, and district. Age- and sex-disaggregated population data were from the 2012 Socio-Economic and Caste Census.

Estimating IFR

Estimating the number of infections. We estimated the number of state-wide infections associated with measured seroprevalence in three steps. First, we calculated positive test rate by district-age-sex group, separately for each kit. Positive test rate was estimated by regressing an indicator for positive result on district-age-sex group indicators, clustering standard errors within the randomly sampled clusters. Seroprevalence sample collection was stratified by district, health unit district (HUD), then cluster; within clusters, age and sex of test participants was random. Thus we take the positive test rate for each district-age-sex group as representative.

Second, we adjusted for test inaccuracies for each kit, using the Rogan-Gladen correction (Rogan and Gladen, 1978) and the manufacturer-provided sensitivity and specificity. In a sensitivity check, we utilized the lowest estimated sensitivity and corresponding specificity, from any manufacturer-conducted or independent analyses of each kit (Figure 7). Independent analysis of the iFlash kit from Shenzhen YHLO Biotech estimated sensitivity of 93% (95% CI: 84 to 97) and specificity of 92% (85 to 97) (Plebani et al., 2020). FDA evaluation of the Vitros kit from Ortho-Clinical Diagnostics suggests 100% sensitivity (95% CI: 88 to 100) and 100% specificity (95 to 100) (USFDA, 2020), while other analysis estimated a sensitivity of 98% (92 to 100) and specificity of 97% (85 to 100) (Theel et al., 2020). Note that, unlike in Mumbai and Karnataka, the minimum sensitivity of the kits in Tamil Nadu had lower corresponding specificity, leading to lower overall seroprevalence estimates. In the district in which both kits were used, kit-specific seroprevalence estimates were averaged, using proportion of sample size (by age-sex group) as the weight.

Third, we estimated number of infections in each district-age-sex group by multiplying seroprevalence rate by population. Age- and sex-disaggregated population data was available for census districts. Finally, estimated state-wide infections by age-sex group were calculated by simply summing over all districts.

Estimating number of deaths in each demographic group. As in Mumbai and Karnataka, we matched the estimated number of infections calculated in each district to the number of deaths recorded in administrative data two days after the last date of seroprevalence surveying. We test sensitivity to alternative assumptions by measuring cumulative deaths 1 week and 2 weeks after the main date (Figure 3). As explained in the supplement sections on Mumbai and Karnataka, these are all plausible over-estimates of deaths associated with the measured seroprevalence level. Cumulative

deaths in each demographic group were measured up to the specified date. Cumulative deaths were measured from March through December, a longer span than in other locations. This may over-estimate deaths, and therefore over-estimate IFR, if infected individuals gradually become seronegative after recovery. Available evidence suggests that antibody loss varies significantly with symptom severity ((Ripperger et al., 2020; Ibarrondo et al., 2020; Long et al., 2020)). Because we cannot precisely estimate antibody loss rates across the population, and because IFR estimates in Tamil Nadu are the lowest across the four locations, we simply note that, given available data, our IFR estimates are conservatively high.

Seroprevalence surveying lasted longer than three weeks in 6 out of 37 districts. In these districts, there is a risk that seroprevalence in the population changed during sample collection. During a period of increasing pandemic intensity, this may under-estimate seroprevalence, over-estimating IFR. As a sensitivity check, we limit analysis of both seroprevalence and deaths to the 31 districts in which seroprevalence sample collection was less than three weeks (Figure 8).

Age- and sex-specific IFRs were estimated as the proportion of state-wide deaths divided by estimated infections. Standard errors reflect propagation of error from the HUD-age-sex estimates of positive test rates.

eFigure 1

Mumbai: sensitivity analysis using number of COVID deaths from 1 and 2 weeks after date of deaths in main estimation

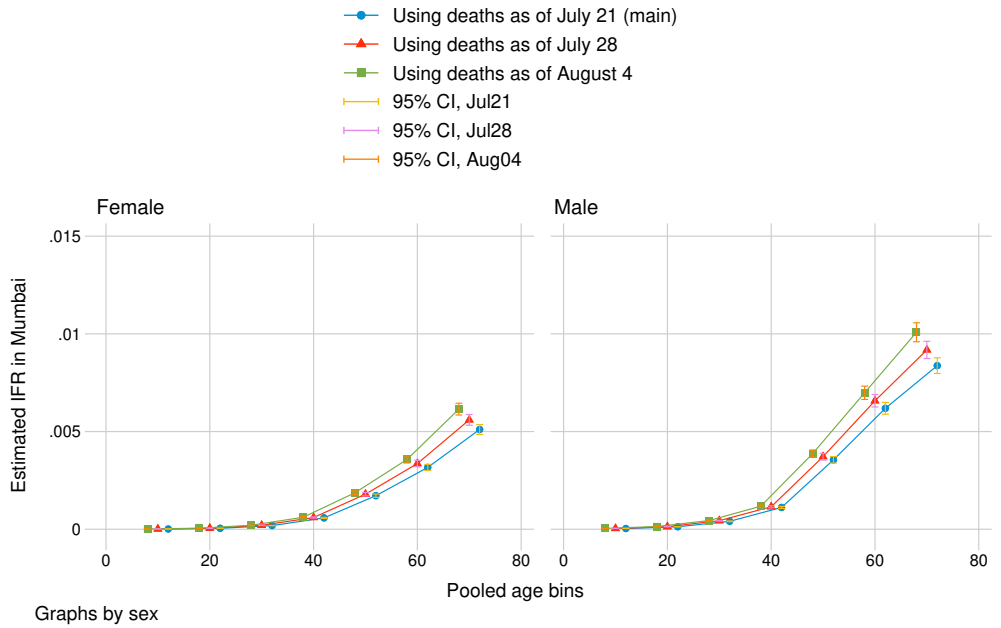

"Date of death" refers to the day on which we measured cumulative deaths as reported by the city government (BMC). The main date specification measured deaths two days after the end of seroprevalence sample collection. Graphs by sex with 95% confidence intervals. Standard errors reflect propagation of error from design-based uncertainty of seroprevalence estimates. IFRs are calculated in age bins 0-19, 20-29, ... 60-69, and 70+.

eFigure 2

Karnataka: sensitivity analysis using number of COVID deaths from 1 and 2 weeks after date of deaths in main estimation

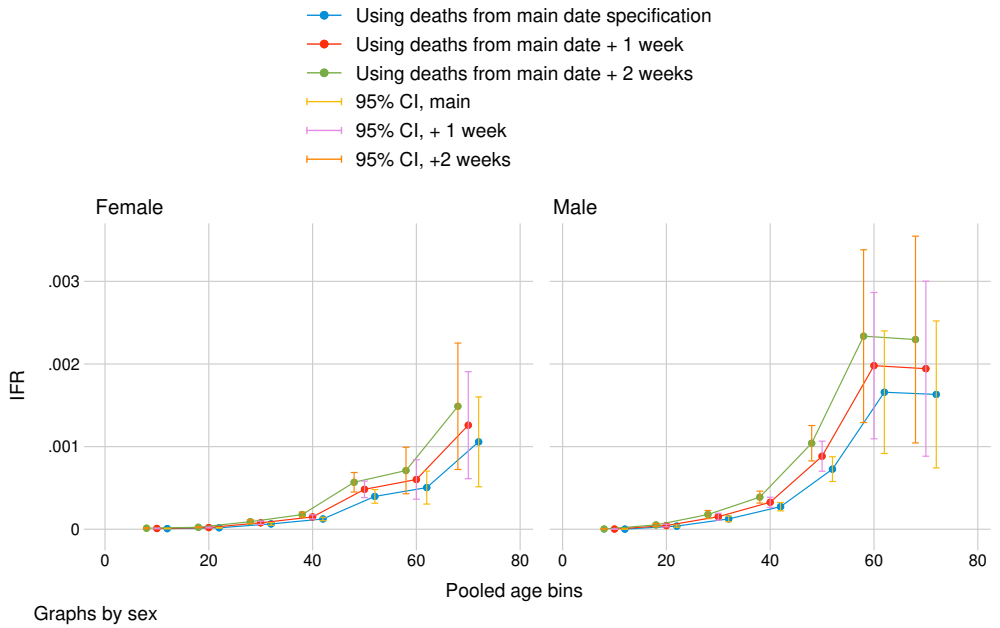

"Date of death" refers to the date on which we measured cumulative COVID-19 deaths. Main date of specification was determined separately for each sampled region as two days after the median date of sample collection. Graphs by sex with 95% confidence intervals. Standard errors reflect propagation of error from design-based uncertainty of seroprevalence estimates. IFRs are calculated in age bins 0-9, ... 60-69, and 70+.

eFigure 3

Tamil Nadu: sensitivity analysis using number of COVID deaths from 1 and 2 weeks after date of deaths in main estimation

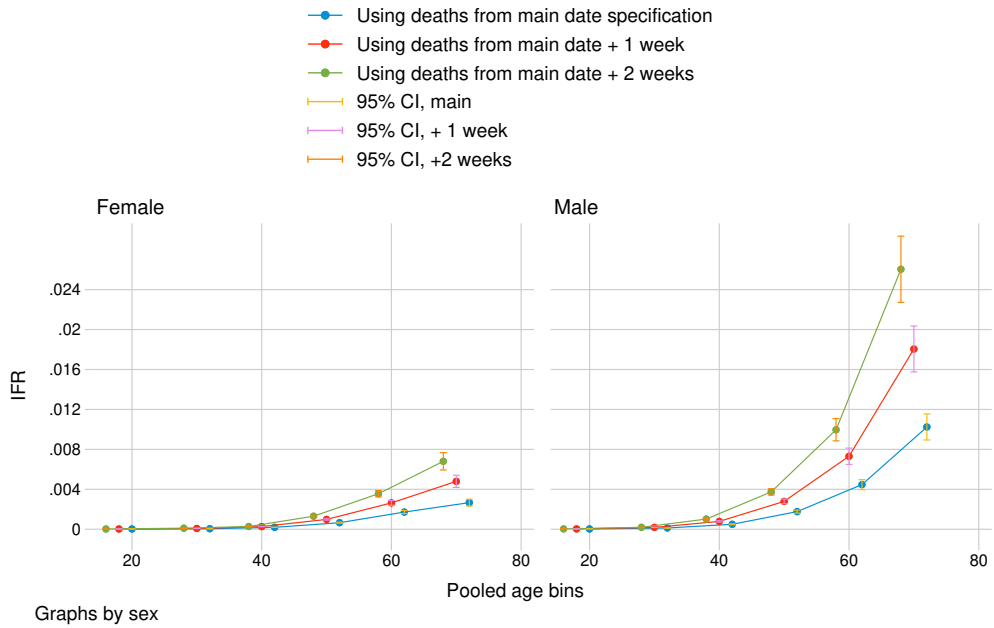

"Date of death" refers to the date on which we measured cumulative COVID-19 deaths. Main date of specification was determined separately for each sampled district (N = 37) as two days after the last date of sample collection. Graphs by sex with 95% confidence intervals. Standard errors reflect propagation of error from uncertainty in estimating positive test rate by HUD-age-sex group. IFRs are calculated in age bins 18-29, 30-39 ... 60-69, and 70+.

eFigure 4
Mumbai:
sensitivity analysis, using alternative estimate of seroprevalence and different interpolation method

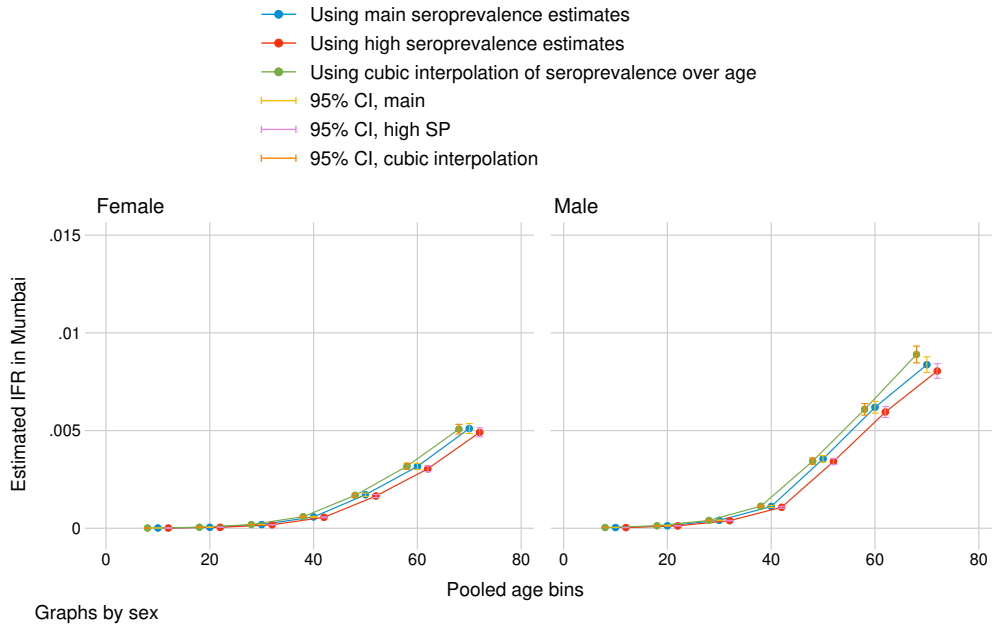

"Main seroprevalence estimates" use midpoint sensitivity estimate of the Abbott antibody test to calculate seroprevalence from seropositivity in sampled wards, then interpolates seroprevalence to finer age bins with inverse distance weighting (IDW). "High seroprevalence estimates" use minimum sensitivity of the Abbott test to calculate seroprevalence from seropositivity and IDW interpolation. The final sensitivity analysis uses midpoint sensitivity, but piecewise cubic Hermite interpolation to estimate seroprevalence in finer bins. Graphs by sex with 95% confidence intervals. Standard errors reflect propagation of error from design-based uncertainty of seroprevalence estimates. IFRs are calculated in age bins 0-19, 20-29, ... 60-69, and 70+.

eFigure 5

Karnataka: sensitivity analysis isolating Bangalore from other sampled regions

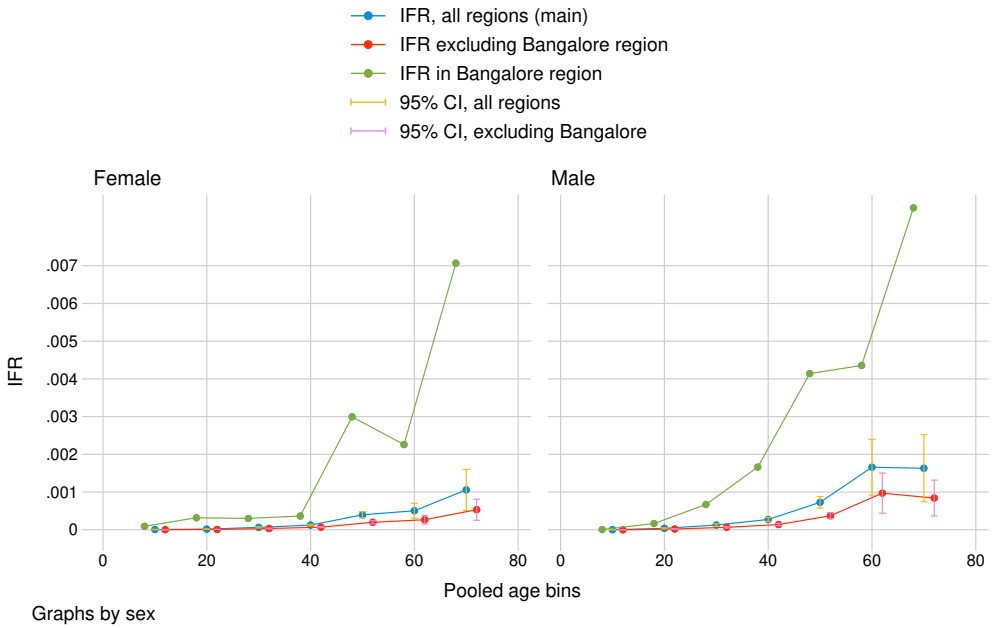

IFRs in main specification are calculated by pooling seroprevalence and death estimates from all five sampled regions of Karnataka. IFRs excluding Bangalore pool from the four remaining regions. Graphs by sex with 95% confidence intervals. Standard errors reflect propagation of error from design-based uncertainty of seroprevalence estimates. Confidence intervals are not reported for Bangalore due to small sample size, and age-specific estimated IFRs in Bangalore should not be interpreted as conclusive. IFRs are calculated in age bins 0-9, ... 60-69, and 70+.

eFigure 6
Karnataka:
sensitivity analysis using piecewise cubic Hermite interpolation to estimate age bin share of deaths

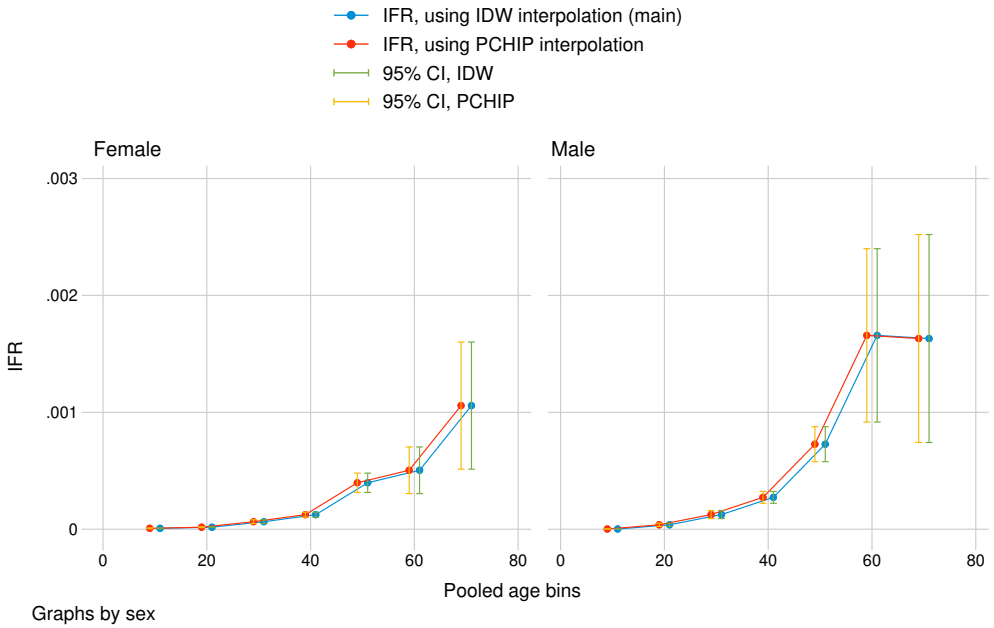

Government reports provide age-shares of deaths in age bins of the form 11-20, 21-30, etc. To match seroprevalence estimates, we interpolate age-shares of deaths in the form 10-19, 20-29, etc. Main specification uses the inverse distance weighted average (IDW) to interpolate age shares. sensitivity analysis uses piecewise cubic Hermite interpolation. Interpolation was done with Stata package mipolate. Graphs by sex with 95% confidence intervals. Standard errors reflect propagation of error from design-based uncertainty of seroprevalence estimates. Confidence intervals are not reported for Bangalore due to small sample size, and age-specific estimated IFRs in Bangalore should not be interpreted as conclusive. IFRs are calculated in age bins 0-9, ... 60-69, and 70+.

eFigure 7

Tamil

Nadu: sensitivity analysis using minimum sensitivity and corresponding specificity of immunoassays.

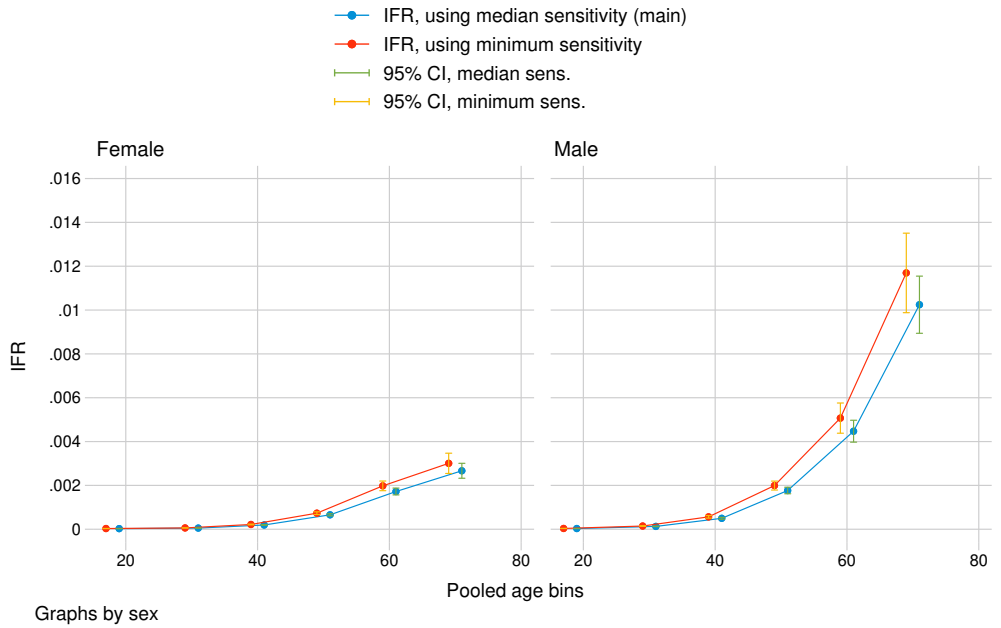

Two kits were used to evaluate seropositivity. Seroprevalence rate was calculated from the seropositivity rate using the Rogan-Gladen correction for imperfect test sensitivity and specificity. Main estimation used the manufacturer-provided sensitivity and corresponding specificity of the kits. The robustness check uses the lowest estimated sensitivity of both kits, which was the manufacturer-provided estimate for the Ortho-Clinical kit. Graphs by sex with 95% confidence intervals. Standard errors reflect propagation of error from uncertainty in estimating positive test rate by HUD-age-sex group. IFRs are calculated in age bins 18-29, 30-39 ... 60-69, and 70+.

eFigure 8

Tamil Nadu: sensitivity analysis excluding districts where sample collection duration exceeded 3 weeks

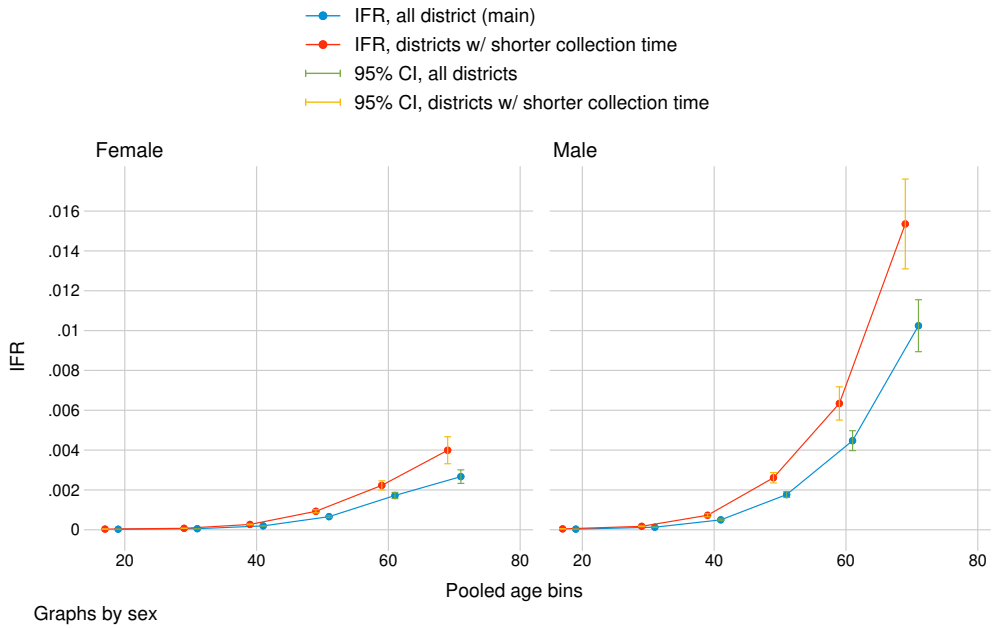

IFRs in main specification are calculated by pooling seroprevalence and death estimates from all 37 districts of Tamil Nadu. IFRs estimated from districts with shorter collection time exclude 6 districts where seroprevalence surveying lasted longer than three weeks. Graphs by sex with 95% confidence intervals. Standard errors reflect propagation of error from uncertainty in estimating positive test rate by HUD-age-sex group. IFRs are calculated in age bins 18-29, 30-39 ... 60-69, and 70+.

eFigure 9

Age-sex cohorts' share of positive cases from sampled wards in Mumbai seroprevalence survey

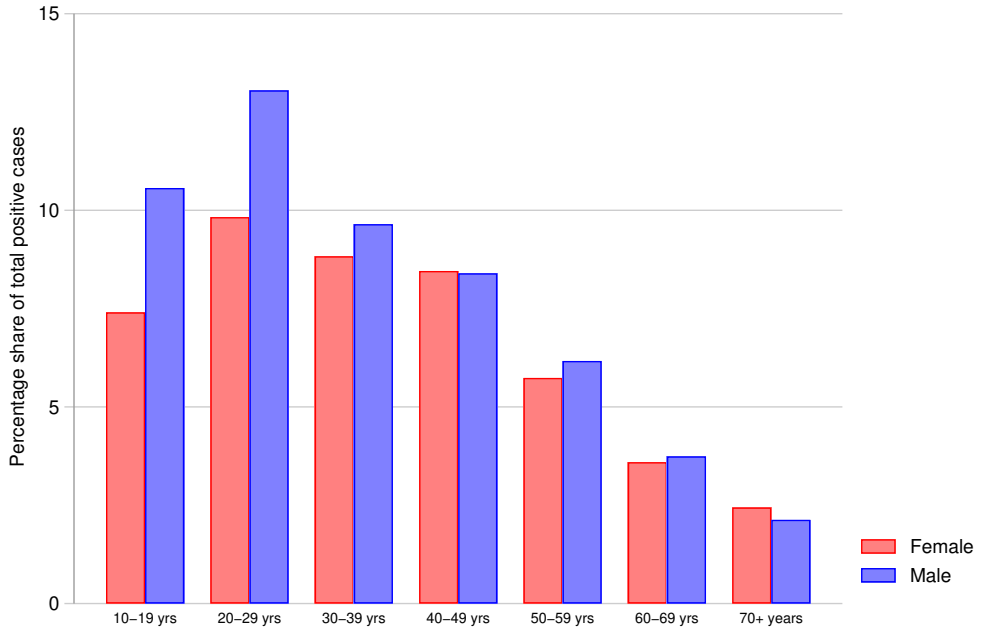

"Total positive cases" refers to the estimated number of total infections in Mumbai, multiplying age- and sex-specific seroprevalence rate by group population, summed across age-sex groups and wards. The age- and sex-share of total cases refers to estimated number of infections in age-sex group *ag*, divided by estimated total infections. Age bins are 0-19, 20-29, ...60-69, and 70+.

1 Supplementary Tables

eTable 1
Zone-wise case multipliers for main and higher seroprevalence estimates based on sampled wards

		No. infections			γ_z	
Ward	*Zone*	*BMC report*	*main SP*	*high SP*	*main SP*	*high SP*
(1)	(2)	(3)	(4)	(5)	(6)	(7)
F North	City	4,017	190,652	211,835	47.6	52.3
M West	Eastern	2,965	139,791	155,322	47.5	52.9
R North	Western	2,421	145,413	161,569	60.6	66.4

"Number of infections, main SP" refers to the estimated seroprevalence (using the midpoint estimated sensitivity of the antibody test) multiplied by population in each sampled ward. "Number of infections, high SP" uses lowest bound sensitivity of the antibody test. Case multiplier "γ_z, main SP" (Column 6) was calculated by dividing Column 4 by Column 3. "γ_z, high SP" (Column 7) was calculated by dividing Column 5 by Column 3. Main SP indicates seroprevalence estimated from midpoint of two published estimates of sensitivity of the antibody test. High SP indicates seroprevalence was estimated using the minimum sensitivity and maximum specificity of the antibody test, generating a upper-bound estimate.

eTable 2
Karnataka: duration of sample collection by region

Region	Duration of sample collection (days)	Dates of sample collection
Bangalore	73	June 17 – August 29
Mysore	18	August 3 – August 21
Kannada	16	August 6 – August 21
Belgaum	17	July 8 – July 25
Gulbarga	10	July 21 – July 31

eTable 3
Mumbai: summary statistics used in calculating IFR

	Seroprev. sample size		Seroprev. rate		No. deaths	
Age	Male	Female	Male	Female	Male	Female
(1)	(2)	(3)	(4)	(5)	(6)	(7)
10–19	210	166	0.339	0.573	14	7
20–29	642	561	0.323	0.555	59	32
30–39	946	897	0.344	0.476	168	90
40–49	929	811	0.428	0.502	454	245
50–59	750	605	0.403	0.531	983	530
60–69	424	307	0.441	0.494	1094	589
70–89	153	88	0.503	0.397	1000	539

Columns 2 and 3 are the number of participants in the seroprevalence survey. Columns 4 and 5 reflect the city-wide seroprevalence rate, adjusted for antibody test sensitivity and specificity. Because we allowed seroprevalence rate to vary across wards, seroprevalence was calculated as number of estimated infections divided by population. Columns 6 and 7 are the number of deaths reported by the city government, split by gender with the assumption that deaths were 65% male, 35% female. See Materials and Methods for details.

eTable 4

Karnataka: summary statistics used in calculating IFR

	Seroprev. sample size		Seroprev. rate		No. deaths	
Age	Male	Female	Male	Female	Male	Female
(1)	(2)	(3)	(4)	(5)	(6)	(7)
10–19	28	30	0.503	0.430	5	14
20–29	84	86	0.342	0.539	59	41
30–39	84	137	0.443	0.388	191	85
40–49	178	175	0.533	0.516	406	168
50–59	129	127	0.516	0.513	687	359
60–69	59	41	0.367	0.474	801	326
70–89	19	19	0.468	0.485	549	321

Columns 2 and 3 are the number of participants in the seroprevalence survey. Columns 4 and 5 reflect the state-wide seroprevalence rate, adjusted for antibody test sensitivity and specificity. Columns 6 and 7 are the number of deaths reported by the state government. See Materials and Methods for details.

eTable 5

Tamil Nadu: summary statistics used in calculating IFR

	Seroprev. sample size		Seroprev. rate		No. deaths	
Age	Male	Female	Male	Female	Male	Female
(1)	(2)	(3)	(4)	(5)	(6)	(7)
18–29	2267	3025	0.292	0.242	56	41
30–39	1794	3576	0.268	0.306	184	90
40–49	1719	3041	0.276	0.295	629	259
50–59	1475	2340	0.284	0.296	1619	614
60–69	1229	1488	0.261	0.249	2510	923
70–89	742	659	0.232	0.258	3029	882

Columns 2 and 3 are the number of participants in the seroprevalence survey. Columns 4 and 5 reflect the state-wide seroprevalence rate, adjusted for antibody test sensitivity and specificity. Because we calculated seroprevalence and corresponding deaths using different dates for different districts, seroprevalence was calculated as total infections across district at time of seroprevalence data collection, divided by population. Columns 6 and 7 are the number of deaths reported by the state government, summed across districts at the time of seroprevalence data collection. See Materials and Methods for details.

eTable 6

Bihar male migrants: summary statistics used in calculating IFR

Age	No. infected	% successfully tracked	No. deaths
(1)	(2)	(3)	(4)
10–19	568	0.674	0
20–29	1472	0.628	6
30–39	989	0.670	12
40–49	543	0.602	5
50–59	189	0.667	3
60–69	69	0.681	2
70–89	13	0.615	1

The table summarizes the group used for analysis: randomly sampled male migrants. Column 2 is the number of men in the sample, who were all infected. Column 3 is the percentage of infected men for whom trackers successfully confirmed an outcome: either recovery or death. Column 4 is the number of confirmed deaths.

References

Bryan, Andrew, Gregory Pepper, Mark H. Wener, Susan L. Fink, Chihiro Morishima, Anu Chaudhary, Keith R. Jerome, Patrick C. Mathias, and Alexander L. Greninger, "Performance Characteristics of the Abbott Architect SARS-CoV-2 IgG Assay and Seroprevalence in Boise, Idaho," *Journal of Clinical Microbiology*, 2020, *58* (8).

Chaudhuri, Susmita, Ramachandran Thiruvengadam, Souvick Chattopadhyay, Farha Mehdi, Pallavi Kshetrapal, Tripti Shrivastava, Bapu Koundinya Desiraju, Gaurav Batra, Gagandeep Kang, and Shinjini Bhatnagar, "Comparative evaluation of SARS-CoV-2 IgG assays in India," *Journal of Clinical Virology*, October 2020, *131*.

CMO-PRC, "Pre-release cm-243: Directions for random testing," May 2020.

Debroy, Sumitra, "Men account for 65% of Mumbai's 6,000+ Covid deaths, CFR high at 6.1%: BMC," *The Times of India*, August 2020.

Deshingkar, Priya, Rajiv Khandelwal, and John Farrington, "Support for migrant workers: The missing link in India's development," Technical Report, Overseas Development Institute September 2008.

Ibarrondo, F. Javier, Jennifer A. Fulcher, David Goodman-Meza, Julie Elliott, Christian Hofmann, Mary A. Hausner, Kathie G. Ferbas, Nicole H. Tobin, Grace M. Aldrovandi, and Otto O. Yang, "Rapid Decay of Anti–SARS-CoV-2 Antibodies in Persons with Mild Covid-19," *New England Journal of Medicine*, September 2020, *383* (11). Publisher: Massachusetts Medical Society pages = 1085–1087.

Laxminarayan, Ramanan, Brian Wahl, Shankar Reddy Dudala, K. Gopal, Chandra Mohan B, S. Neelima, K. S. Jawahar Reddy, J. Radhakrishnan, and Joseph A. Lewnard, "Epidemiology and transmission dynamics of COVID-19 in two Indian states," *Science*, November 2020, *370* (6517), 691–697.

Lewnard, Joseph A., Vincent X. Liu, Michael L. Jackson, Mark A. Schmidt, Britta L. Jewell, Jean P. Flores, Chris Jentz, Graham R. Northrup, Ayesha Mahmud, Arthur L. Reingold, Maya Petersen, Nicholas P. Jewell, Scott Young, and Jim Bellows, "Incidence, clinical outcomes, and transmission dynamics of severe coronavirus disease 2019 in California and Washington: prospective cohort study," *BMJ*, May 2020, *369*.

Linton, Natalie M., Tetsuro Kobayashi, Yichi Yang, Katsuma Hayashi, Andrei R. Akhmetzhanov, Sung-Mok Jung, Baoyin Yuan, Ryo Kinoshita, and Hiroshi Nishiura, "Incubation Period and Other Epidemiological Characteristics of 2019 Novel Coronavirus Infections with Right Truncation: A Statistical Analysis of Publicly Available Case Data," *Journal of Clinical Medicine*, February 2020, *9* (2).

Long, Quan-Xin, Xiao-Jun Tang, Qiu-Lin Shi, Qin Li, Hai-Jun Deng, Jun Yuan, Jie-Li Hu, Wei Xu, Yong Zhang, Fa-Jin Lv, Kun Su, Fan Zhang, Jiang Gong, Bo Wu, Xia-Mao Liu, Jin-Jing Li, Jing-Fu Qiu, Juan Chen, and Ai-Long Huang, "Clinical and immunological assessment of asymptomatic SARS-CoV-2 infections," *Nature Medicine*, August 2020, *26* (8), 1200–1204.

Malani, Anup, Daksha Shah, Gagandeep Kang, Gayatri Nair Lobo, Jayanthi Shastri, Manoj Mohanan, Rajesh Jain, Sachee Agrawal, Sandeep Juneja, Sofia Imad, and Ullas Kolthur-Seetharam, "Seroprevalence of SARS-CoV-2 in slums versus non-slums in Mumbai, India," *The Lancet Global Health*, November 2020, *0* (0).

Mohanan, Manoj, Anup Malani, Kaushik Krishnan, and Anu Acharya, "Prevalence of SARS-CoV-2 in Karnataka, India," *JAMA*, February 2021.

Plebani, Mario, Andrea Padoan, Davide Negrini, Benedetta Carpinteri, and Laura Sciacovelli, "Diagnostic performances and thresholds: The key to harmonization in serological SARS-CoV-2 assays?," *Clinica Chimica Acta; International Journal of Clinical Chemistry*, October 2020, *509*, 1–7.

Ripperger, Tyler J., Jennifer L. Uhrlaub, Makiko Watanabe, Rachel Wong, Yvonne Castaneda, Hannah A. Pizzato, Mallory R. Thompson, Christine Bradshaw, Craig C. Weinkauf, Christian Bime, Heidi L. Erickson, Kenneth Knox, Billie Bixby, Sairam Parthasarathy, Sachin Chaudhary, Bhupinder Natt, Elaine Cristan, Tammer El Aini, Franz Rischard, Janet Campion, Madhav Chopra, Michael Insel, Afshin Sam, James L. Knepler, Andrew P. Capaldi, Catherine M. Spier, Michael D. Dake, Taylor Edwards, Matthew E. Kaplan, Serena Jain Scott, Cameron Hypes, Jarrod Mosier, David T. Harris, Bonnie J. LaFleur, Ryan Sprissler, Janko Nikolich-Žugich, and Deepta Bhattacharya, "Orthogonal SARS-CoV-2 Serological Assays Enable Surveillance of Low-Prevalence Communities and Reveal Durable Humoral Immunity," *Immunity*, November 2020, *53* (5), 925–933.e4.

Rogan, W. J. and B. Gladen, "Estimating prevalence from the results of a screening test," *American Journal of Epidemiology*, January 1978, *107* (1), 71–76.

Shenzhen YHLO Biotech No. Ltd., "Customer Notification: Sensitivity and Specificity of iFlash-SARS-CoV-2 and IgM kits from Clinical Trials.," Technical Report 2020.

Stringhini, Silvia, Ania Wisniak, Giovanni Piumatti, Andrew S. Azman, Stephen A. Lauer, Hélène Baysson, David De Ridder, Dusan Petrovic, Stephanie Schrempft, Kailing Marcus, Sabine Yerly, Isabelle Arm Vernez, Olivia Keiser, Samia Hurst, Klara M. Posfay-Barbe, Didier Trono, Didier Pittet, Laurent Gétaz, François Chappuis, Isabella Eckerle, Nicolas Vuilleumier, Benjamin Meyer, Antoine Flahault,

Laurent Kaiser, and Idris Guessous, "Seroprevalence of anti-SARS-CoV-2 IgG antibodies in Geneva, Switzerland (SEROCoV-POP): a population-based study," *The Lancet*, August 2020, *396* (10247), 313–319.

Theel, Elitza S., Julie Harring, Heather Hilgart, and Dane Granger, "Performance Characteristics of Four High-Throughput Immunoassays for Detection of IgG Antibodies against SARS-CoV-2," *Journal of Clinical Microbiology*, July 2020, *58* (8).

USFDA, U.S. Food and Drug Administration, "Serology Test Evaluation Report for "Architect i1000 SARS-CoV-2 IgG" from Abbott," Technical Report 2020.